PHILOSOPHICAL TRANSACTIONS OF THE ROYAL SOCIETY A MATHEMATICAL, PHYSICAL & ENGINEERING SCIENCES

Versatile femtosecond laser sources for time–resolved studies: configurations and characterizations

W. Sibbett, D. T. Reid and M. Ebrahimzadeh

Phil. Trans. R. Soc. Lond. A 1998 **356**, 283-296
doi: 10.1098/rsta.1998.0165

The Royal Society

Versatile femtosecond laser sources for time-resolved studies: configurations and characterizations

By W. Sibbett, D. T. Reid and M. Ebrahimzadeh

School of Physics and Astronomy, University of St Andrews, North Haugh, St Andrews, Fife KY16 9SS, UK

The generation of tunable ultrashort laser pulses in different regions of the optical spectrum has particular significance for the study of the rapid events that arise in photochemistry and photobiology. High-resolution techniques which use such pulses to probe transient phenomena require high-repetition-rate sources which can operate over extended wavelength regions in the visible and infrared. Dramatic progress in the development of ultrafast sources has taken place during the 1990s and we present here a review of those which now represent practical tools for time-resolved studies and describe powerful characterization techniques for the pulses which they produce.

Keywords: tunable femtosecond lasers; frequency downconversion; optical parametric oscillators; ultrashort-pulse diagnostics

1. Source specifications for time-resolved studies

The study of ultrafast processes in chemistry and biology has been greatly boosted by the availability of a growing range of broadly tunable ultrashort-pulse laser-based sources. A major driving force behind these source developments in the 1990s has been the discovery of the self-mode-locking (also called the Kerr-lens mode-locking) technique in vibronic lasers (Spence *et al.* 1990, 1991*a*). As a consequence, there has been a burgeoning of readily available options for attractively practical and reliable picosecond/femtosecond sources that are compatible with a wide variety of time-resolved studies in pure and applied science. At the research level, there continues to be a clear motivation towards the further development of increasingly refined lasers and laser-related sources that have the capability of producing ultrashort pulses having enhanced characteristics such as ever shorter durations, greater peak intensities or wider tunability. Importantly, these advances have been complemented by innovative pulse-characterization techniques (Trebino & Kane 1993) such that all of the features of picosecond and femtosecond optical pulses can now be subjected to detailed scrutiny. Taken together, this means that modern time-resolved spectroscopy can exploit novel quantified manipulations such as the synthesized frequency chirping of femtosecond pulses (Kohler *et al.* 1995). Applications of this type serve to illustrate the user-compatibility of self-mode-locked lasers, laser and parametric amplifiers and related specialist diagnostics.

The dynamics of the ultrafast relaxation processes commonly studied using pump-probe techniques are complex and their analysis involves fitting data to the detailed features of the observed temporal response characteristics. In some applications,

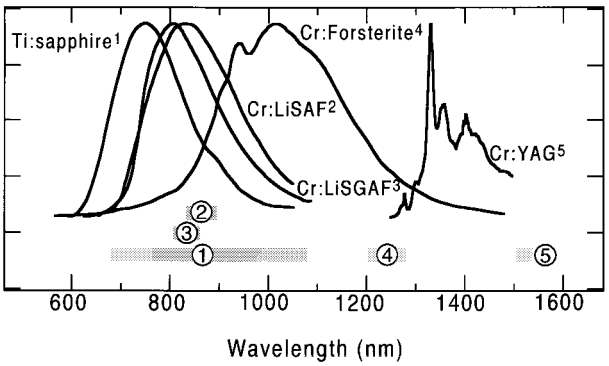

Figure 1. Emission bandwidths for the common vibronic laser materials Ti:sapphire, Cr:LiSAF, Cr:LiSGAF, Cr:Forsterite and Cr:YAG. Wavelength ranges across which femtosecond operation has been demonstrated are shown in grey.

achieving a high signal-to-noise ratio in the measurement of the data is of primary importance and this is only made practicable by using a mode-locked source with a high pulse-repetition rate. Prior to the introduction of the self-mode-locked Ti:sapphire laser (Spence *et al.* 1990, 1991*a*), high repetition-rate sources offered very limited tunability and methods of extending the wavelength coverage of these systems (e.g. continuum generation or optical parametric amplification) reduced the pulse repetition frequencies from around 100 MHz to no more than a few kHz (Knox *et al.* 1984). Operating at high output powers with pulse durations as short as 60 fs and tuning continuously from 670 to 1070 nm, the self-mode-locked Ti:sapphire laser was the first of a new generation of mode-locked lasers based on vibronic gain media (Spence *et al.* 1991*a*). Self-mode-locked femtosecond oscillators have since been demonstrated based on other vibronic laser media such as Cr:forsterite (Seas *et al.* 1992), Cr4+:YAG (Sennaroglu *et al.* 1994), Cr:LiSAF (Evans *et al.* 1992) and Cr:LiSGaF (Yanovsky *et al.* 1995), but Ti:sapphire oscillators remain the most powerful and most broadly tunable high-repetition-rate femtosecond sources available to date. The emission bandwidths for these gain media are illustrated together with that of Ti:sapphire in figure 1, and the tuning of femtosecond lasers based on these materials is also depicted. Generation of high-repetition-rate femtosecond pulses in the visible and ultraviolet has been shown to be readily achievable with Ti:sapphire lasers by using intracavity frequency doubling (Ellingson & Tang 1992) and extracavity sum-frequency mixing (Nebel & Beigang 1991). With the exception of enhancement cavity resonant-doubling techniques, femtosecond frequency downconversion to infrared wavelengths is more complex to implement than upconversion and requires the parametric schemes which are introduced in the remainder of this section.

The high output power of the femtosecond self-mode-locked Ti:sapphire laser made it suitable for the synchronous pumping of singly resonant optical parametric oscillators (OPOs). These devices offer continuous tunability across very wide spectral regions and, using techniques such as quasi-phasematching, the output wavelengths can extend from within the Ti:sapphire emission bandwidth to beyond 5 μm. An OPO can be thought of as a 'photon-splitter', where a high-energy *pump* photon (in this case from a Ti:sapphire laser) is broken into two unequal components. The higher-energy component corresponds to the *signal* wave which is resonated in a high-finesse cavity while the lower-energy portion (the *idler* wave) is allowed to leave the resonator on a single pass. Conversion efficiencies from the pump wave into

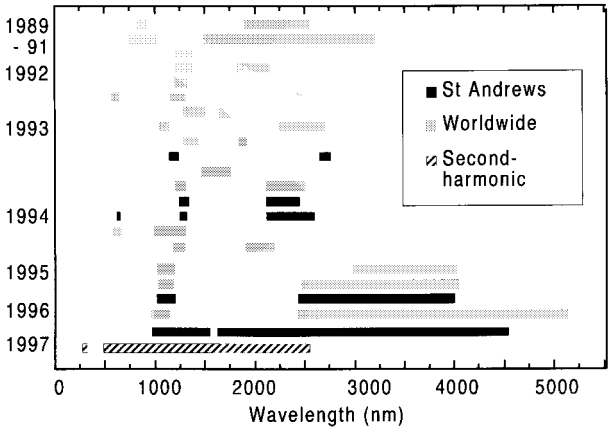

Figure 2. Chronological representation of wavelength tuning demonstrated to date using femtosecond optical parametric oscillators (separate ranges lying on the same horizontal line correspond to tuning from a single system). The results from our laboratory are emphasized in black and are compared to other published results shown in grey. The hatched boxes illustrate the extension of the fundamental OPO wavelengths to the visible and ultraviolet by using frequency doubling.

the signal wave (typical wavelength from 1.0 to 1.6 μm) can approach 50%. The output wavelengths produced by high-repetition-rate femtosecond OPOs are illustrated schematically in figure 2. The wide tunability and high efficiency of femtosecond OPOs makes them ideal for time-resolved studies. The repetition rate of the laser and OPO are exactly matched which means that pump-probe measurements in two well-separated spectral bands are feasible. By utilising frequency doubling (shown as hatching in figure 2), the output of a system based on a Ti:sapphire-pumped OPO can range from the ultraviolet to the mid-infrared with almost continuous tunability and with average powers of several mW to several hundred mW.

Within photobiology and some aspects of photochemistry, the recovery timescales of the photoexcited specimens are such that a very high repetition-rate-pulse source is not suitable for time-resolved studies. In these cases, it is preferable to use either cavity-dumping or amplification schemes as methodologies for enhancing the pulse energies appropriately and of reducing the repetition frequency of the ultrashort-pulse sources. For example, cavity-dumped Ti:sapphire lasers have been shown to be extremely effective sources in the MHz pulse-repetition frequency regimes (Ramaswamy *et al.* 1993; Pshenichnikov *et al.* 1994). Indeed, pulses produced by a Ti:sapphire laser that was cavity dumped at 1 MHz repetition rate have been temporally compressed to durations as short as 5 fs (Baltuska *et al.* 1997).

In the following section, a review is presented of the progress in self-mode-locked laser sources and this is followed by an account of some representative femtosecond OPO sources demonstrated to date in our laboratories. Finally, recent work on simple and novel pulse characterization techniques is presented which has significance for many users of femtosecond-pulse sources.

2. Self-mode-locked femtosecond lasers

The simplicity of the self-mode-locking principle is key in enabling a tunable and efficient high-repetition-rate femtosecond laser to be constructed. The vibronic gain media used in self-mode-locked lasers show a significant intensity dependence of their

refractive indices through the optical Kerr effect. By exploiting this effect, a simple four-mirror resonator can be configured so that the propagation of high peak-power pulses in the cavity is favoured. The absence of any resonant mode-locking elements (e.g. dyes, saturable absorbers) means that the outputs from self-mode-locked lasers are generally tunable across the entire emission bandwidths of the gain media. Practical self-mode-locked lasers, however, often utilise an additional cavity element to initiate mode-locking. This is necessary because the self-mode-locking process is not in general self-starting and requires some form of external perturbation to provide a high-intensity noise-spike or a primitive picosecond pulse which is shortened as it propagates around the laser resonator and becomes the mode-locked pulse. Popular initiation techniques include regenerative acousto-optic modulation (Spence *et al.* 1991*b*; Kafka *et al.* 1992), saturable absorber mirrors (SAMs) (Brovelli *et al.* 1995; Tsuda *et al.* 1995) and moving mirrors (Rizvi *et al.* 1992; Liu *et al.* 1992; Pelouch *et al.* 1992). In the first of these techniques, the oscillator incorporates an acousto-optic modulator which is driven at the cavity frequency (or a harmonic) of the laser resonator using a feedback loop to produce picosecond pulses which are sufficiently short to initiate self-mode-locking. Initiation using semiconductor saturable-absorber mirrors works in an entirely passive manner but is limited to wavelengths within the bandwidth of the saturable absorber and the SAM devices themselves are not yet widely available. The simplest method is to create a noise spike by a small perturbation of a mirror which is sufficient to initiate self-mode-locked operation which remains for several hours.

For optimum ultrashort pulse generation, the group delay (or round-trip period) for the light in the laser cavity should be essentially frequency independent. We can express this group delay as $T_g(\omega)$ and use a Taylor series expansion about a centre frequency ω_c. Thus,

$$T_g(\omega) = \frac{\partial\phi}{\partial\omega}(\omega_c) + \frac{\partial^2\phi}{\partial\omega^2}(\omega_c)\Delta\omega + \frac{1}{2}\frac{\partial^3\phi}{\partial\omega^3}(\omega_c)\Delta\omega^2 + \frac{1}{6}\frac{\partial^4\phi}{\partial\omega^4}(\omega_c)\Delta\omega^3 + \cdots,$$

where ϕ is the total phase change during each cavity trip. This represents the first- to fourth-order dispersion contributions. In a self-mode-locked laser, the second-order dispersion (ie. group velocity) gives rise to a linear chirp and in general this should be small and negative to ensure a stable evolution of femtosecond pulses. It is also important to compensate for the third- and higher-order dispersion contributions so that the best balance can be established between them and the self-phase modulation. For example, by careful control of intracavity dispersion, it has been possible to obtain pulse durations in the 8 fs regime from a self-mode-locked laser having a 2 mm long Ti:sapphire crystal and a pair of fused silica prisms (Zhou *et al.* 1994). However, the absolute minimum pulse duration is determined by the width of the laser emission bandwidth which in the case of Ti:sapphire corresponds to a value of around 3 fs. An alternative method of dispersion compensation uses chirped-dielectric cavity mirrors whose reflected phase has been engineered to provide an intrinsic negative dispersion which is tailored to exactly balance the positive dispersion of the gain medium (Stingl *et al.* 1994). Using this technology, pulse durations of 7.5 fs have been measured directly from a self-mode-locked Ti:sapphire laser in a ring cavity configuration (Xu *et al.* 1996).

The self-mode-locking technique lends itself well to miniaturization of femtosecond lasers because no components are required besides the crystal and cavity mirrors. 105 fs duration pulses have been produced at a repetition-frequency of 1 GHz using

a 15 cm long cavity comprising only a Ti:sapphire laser crystal and a two discrete mirrors (Bouma & Fujimoto 1996). Ultrahigh-repetition-rate sources such as this can be particularly useful for time-resolved studies because of the signal-to-noise advantage which they can offer over lower pulse-repetition-rate systems.

The ability to miniaturize the laser itself only becomes significant when the size of the complete system including the pump source can be downscaled. Until very recently, femtosecond laser sources were pumped using large water-cooled mainframe lasers such as an argon-ion or an arclamp-pumped Nd:YAG laser. New laser materials and new all-solid-state pump sources have allowed dramatic progress to be made in reducing the size of the overall femtosecond laser system. Improvements in the operating lifetime and output power of 810 nm laser diode arrays have enabled the development of diode-based 'minilasers' such as the 527 nm Millennia which is available (Spectra-Physics Lasers) as a direct low-power replacement for argon-ion lasers and consumes a fraction of the bench space and electricity associated with its mainframe equivalent. Using a 5 W Millennia as a pump source we have measured an average power of 900 mW from a femtosecond Ti:sapphire oscillator containing a 10 mm long highly doped crystal. Measurements using this laser have also demonstrated that it exhibits substantially superior amplitude and phase noise characteristics compared to the argon-ion pumped counterpart (Lamb 1996).

Minilaser pumping has also been used in conjunction with Cr^{4+}:YAG to produce a compact femtosecond laser operating in the 1.5 μm region (Valentine *et al.* 1996). The schematic in figure 3 shows an all-solid-state regeneratively initiated self-mode-locked Cr^{4+}:YAG laser used in our laboratory which produces 180 fs duration pulses at an average power of 55 mW and a repetition frequency of 193 MHz (Valentine *et al.* 1996). A compact three-mirror resonator design is used and the intracavity dispersion is minimized by using a prismatic mode-locker as one of the dispersion-compensating prisms within the cavity. The inset in figure 3 shows a typical pulse autocorrelation and spectrum at the operating wavelength of 1510 nm.

A more dramatic reduction in the size of a femtosecond source is possible when the vibronic laser material absorption band includes a suitable laser-diode emission wavelength. Self-mode-locking of diode-laser (AlGaInP) pumped Cr:LiSAF has been investigated extensively (Dymott & Ferguson 1994, 1995; Kopf *et al.* 1994; Critten *et al.* 1996; Tsuda *et al.* 1996; Aoshima *et al.* 1997; Robertson *et al.* 1997) and average output powers as high as 100 mW at 868 nm have been reported in the literature (Falcoz *et al.* 1995) and unpublished figures of 200 mW have been reported elsewhere (Kärtner *et al.* 1996). Direct diode pumping of Cr:LiSGaF has also been reported (Yanovsky *et al.* 1995) with an average mode-locked output power of 35 mW and a pulse duration of 100 fs.

The poor beam quality of many of the higher-power broad-stripe diode lasers makes optimal matching of the pump and cavity modes impractical. By using an optical feedback technique known as self-injection locking, we have been able to obtain a near-diffraction-limited output from a broad-stripe (AlGaInP) diode laser which has enabled us to efficiently pump self-mode-locked Cr:LiSAF (Burns *et al.* 1996) and Cr:LiSGaF lasers. In the cavity geometry shown in figure 4 for the Cr:LiSGaF laser, pumping with a single 670 nm laser-diode at 170 mW produced 12 mW of average power and pulse durations as short as 87 fs at 850 nm (Critten *et al.* 1996). Typical autocorrelation and spectral data are included in the inset in figure 4. The resonator was optimized for low threshold operation and further work has since demonstrated that stable self-mode-locking can be achieved in a Cr:LiSGAF laser for an inci-

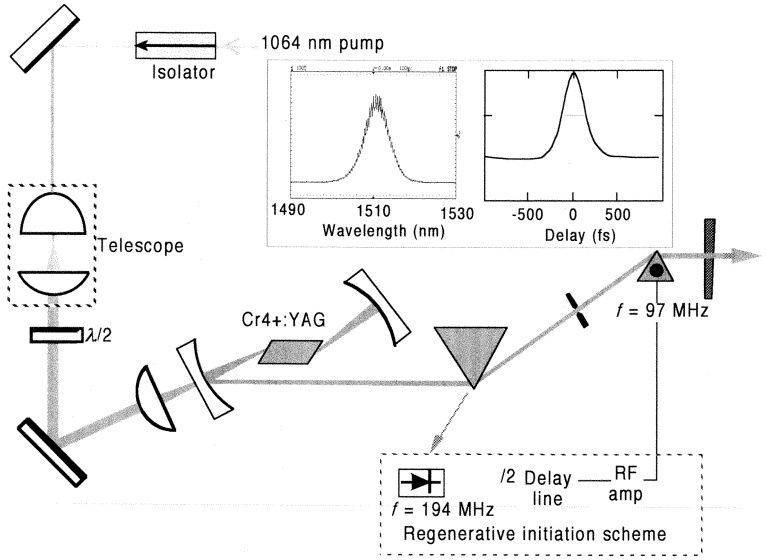

Figure 3. Schematic of a compact all-solid-state self-mode-locked Cr:YAG laser operating at a pulse repetition frequency of 194 MHz. The inset shows a typical spectrum (left) and intensity autocorrelation (right) of the output pulses.

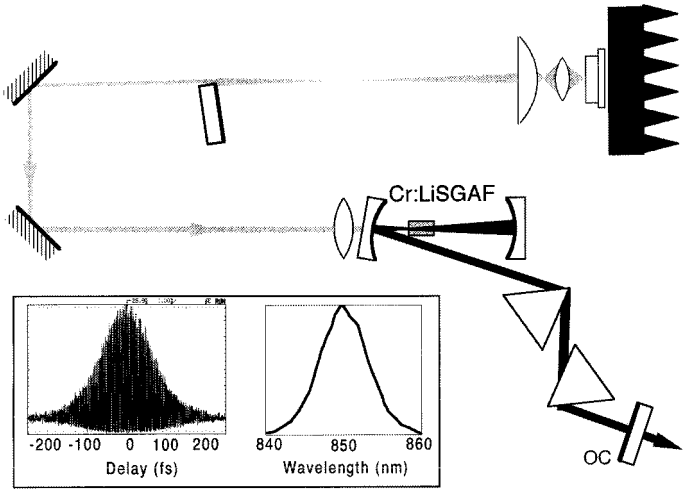

Figure 4. Schematic of a self-mode-locked Cr:LiSGAF laser pumped directly by a single AlGaInP diode laser. The inset shows the interferometric autocorrelation (left) and spectrum (right) of the pulses produced by the laser.

dent pump power of 25 mW with a threshold for femtosecond-pulse generation at just 20 mW. This result is particularly significant because more powerful diffraction-limited narrow-stripe diode lasers are now becoming available and it therefore brings the prospect of increasingly compact and cheap femtosecond laser sources within reach.

A major attribute of self-mode-locked vibronic lasers is their high peak pulse powers. Where necessary, this can be further enhanced at high repetition rates by cavity dumping schemes (Ramaswamy *et al.* 1993; Blatuska *et al.* 1997) or at somewhat lower repetition rates by chirped-pulse amplification techniques (Strickland & Mourou

1985; Zhou *et al.* 1995; Mellish *et al.* 1995). At the terawatt power levels, picosecond and sub-picosecond X-ray pulses can be generated in ultrafast laser-produced plasmas (Murnane *et al.* 1989; Kmetec *et al.* 1992). Thomson scattering from relativistic electron beams (Kim *et al.* 1994) and novel high-harmonic generation have been identified as an effective methodology for the production of XUV, soft X-ray pulses in the femtosecond and possibly attosecond regimes (Corkum 1993; Corkum *et al.* 1994). Consequently, these sources have particular relevance to time-resolved X-ray absorption and diffraction though which either the evolution of chemical reactions or the microscopic processes in biomolecular samples can be observed.

Access to spectral regions in the near- to mid-infrared is gained relatively efficiently by a range of frequency downconversion techniques. The greatest flexibility is offered by optical parametric oscillators that are synchronously pumped by self-mode-locked lasers to provide high optical quality pulses in the picosecond and femtosecond regimes. The latter is the subject matter reviewed in the next section of this paper.

3. Broadly tunable femtosecond optical parametric oscillators

The capacity for wavelength tuning is an essential ingredient of any versatile femtosecond source in photochemistry and photobiology studies and impressive spectral agility is available from a parametric frequency downconversion process. Ultrafast optical parametric amplification (OPA) is only efficient for high-energy amplified femtosecond pulses which, while suitable for some applications, may not be as suitable as the continuous sequence of identical pulses produced by an optical parametric oscillator (OPO). In character and functionality an ultrafast OPO has many similarities to a femtosecond laser and the output beam is coherent and diffraction limited. The OPO is synchronously pumped, most frequently by a self-mode-locked Ti:sapphire laser operating at a pulse repetition frequency of close to 80 MHz, and its resonator must therefore be period matched to that of the pump laser. Unlike a laser, the OPO has no population inversion and therefore no gain lifetime and consequently the optical cavity lengths must be identical to within 1–2 μm. In practice, this degree of accuracy is not prohibitive and, once properly synchronized, the OPO can remain in operation indefinitely without any form of electronic stabilization.

The output wavelengths from an OPO depend critically on the particular nonlinear crystal used, its angle, temperature and the pump wavelength. The signal and idler outputs are determined by the *phasematching* conditions for the pump, signal and idler waves which require conservation of energy ($\hbar\omega_s + \hbar\omega_i = \hbar\omega_p$) and vector momentum ($\hbar\boldsymbol{k}_s + \hbar\boldsymbol{k}_i = \hbar\boldsymbol{k}_p$). The specific variation of the refractive index of a nonlinear crystal with temperature, polarization, wavelength and angle of incidence defines its tuning behaviour and this is conveniently represented by phasematching curves which depict the output wavelengths as a function of these variable parameters. Figure 5 presents a phasematching diagram for the nonlinear crystal $KTiOAsO_4$ (KTA) which we have demonstrated in a femtosecond OPO (Reid *et al.* 1997*a*). The open and closed symbols are experimental tuning data at pump wavelengths of 816 and 846 nm, respectively, for the signal (circles) and idler (squares) outputs. The propagation angle θ_p is measured inside the crystal relative to the optical z-axis and the OPO tunes from 1.03 to 1.2 μm and 2.5–4.1 μm for an angular variation of only 4°. A schematic of the OPO cavity is shown in figure 6 together with representative

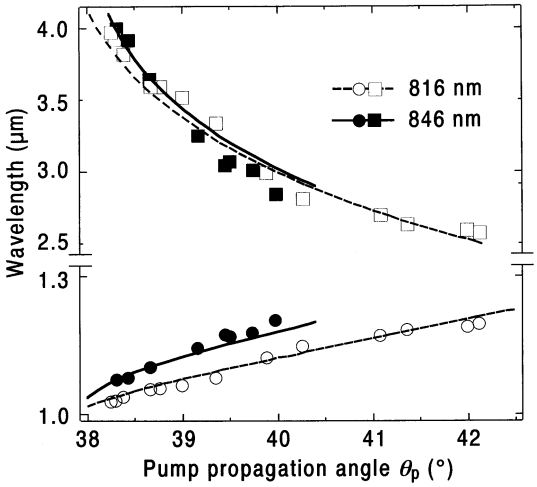

Figure 5. Experimental angle tuning of the signal (circles) and idler (squares) output of a Ti:sapphire-pumped KTA OPO for pump wavelengths of 816 nm (open symbols) and 846 nm (filled symbols). Tuning predicted using refractive index data for KTA is shown for the two pump wavelengths as a solid line (846 nm) and a dashed lined (816 nm).

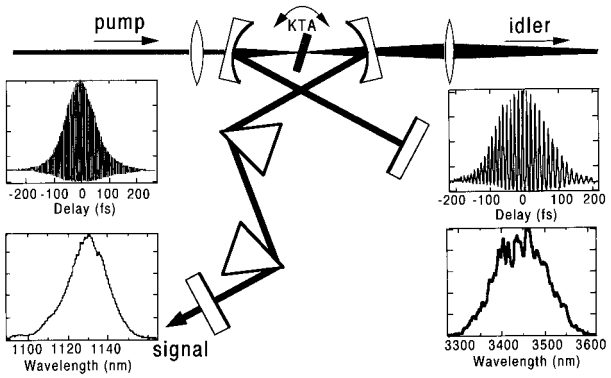

Figure 6. Cavity schematic of the Ti:sapphire-pumped KTA OPO illustrating the direction of crystal angle tuning. Autocorrelation and spectral data are shown for the 1.1 μm signal pulses from the OPO (left) and the 3.5 μm idler pulses (right).

signal and idler pulse measurements in the near- and mid-infrared. The maximum powers in the signal at 1.2 μm and idler at 2.5 μm were 80 and 110 mW, respectively.

Traditional crystals such as KTA are phasematched by relying on the crystal birefringence to compensate for wavelength dispersion and thus meet the phasematching conditions. Some attractive materials for OPO applications (e.g. those with high nonlinearity or wide transparency) cannot be used because they lack sufficient birefringence to allow conventional phasematching to be achieved in the wavelength regions of interest. The suitability of periodic poling (Fejer *et al.* 1992) has recently been demonstrated as a scheme whereby any three-wave interaction can be phasematched irrespective of birefringence. The pump, signal and idler waves are identically polarized in a direction chosen to exploit the highest nonlinearity in the crystal. Efficient exchange of energy from the pump to the signal and idler occurs over the coherence length for the interaction which is typically 10–20 μm. Beyond this length backconversion occurs unless the polarity of the nonlinear coefficient is reversed.

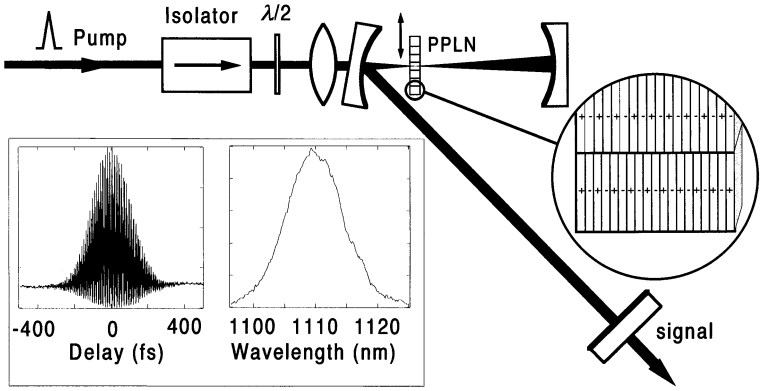

Figure 7. Cavity schematic of the Ti:sapphire-pumped PPLN OPO including a magnified representation of two of the periodically poled gratings fabricated on the crystal. The inset shows a typical autocorrelation and spectrum from the OPO operated with dispersion compensation (not shown).

By periodically reversing the sign of the nonlinearity at intervals of one coherence length efficient conversion is maintained. Modifying the exact period of this grating structure changes the signal and idler wavelengths which are phasematched. In some preliminary studies we have demonstrated a femtosecond OPO using periodically poled lithium niobate (PPLN) and have achieved tuning from 975 nm to 1.54 μm in the signal band and 1.67–4.55 μm for the idler by using a range of gratings with different periods fabricated on a single crystal as illustrated in the schematic of figure 7. Lithium niobate is sensitive to photorefractive damage at room temperature (Myers *et al.* 1995) and, while we have operated the OPO under these conditions, stable operation was ensured by maintaining the crystal temperature at 100 °C using a miniature oven (not shown). The maximum signal and idler powers recorded were 90 and 50 mW, respectively, and temporal and spectral measurements for the signal pulses are shown in the inset in figure 7. Periodic poling is a powerful technique because it allows the highest nonlinear coefficient in a material to be exploited and consequently crystals with very high parametric gains can be fabricated. The PPLN OPO reported here has operated with only 40 mW of average pump power and such a low threshold has important implications for the next generation of compact tunable femtosecond sources which are likely to be based on directly diode-pumped Cr:LiSAF or Cr:LiSGaF lasers.

The requirement for synchronous pumping has, until recently, restricted the repetition rate of femtosecond OPOs to that of the pump laser. Using a novel resonator geometry shown in figure 8 we have increased the pulse repetition frequency to four times the pump laser frequency (Reid *et al.* 1997*b*). The nonlinear crystal is $RbTiOAsO_4$ (RTA) and one surface is prepared with a dichroic coating which is highly reflective at the resonant signal wavelength and highly transmissive at the pump wavelength. The length of the resonator is only 43 cm, four times shorter than that of the pump laser, and, after amplification by a pump pulse, the signal pulse makes four roundtrips of the cavity before meeting the subsequent pump pulse. The signal wavelength is tunable from 1.2 to 1.4 μm by changing only the pump wavelength and the pulse-repetition frequency is 344 MHz. The inset in figure 8 shows the signal pulse sequence recorded on a fast photodiode. The cavity geometry uniquely facilitates very tight focusing to be achieved which has enabled us to produce up to 600 mW at 1.25 μm at a repetition frequency of 86 and 170 mW in each of the signal

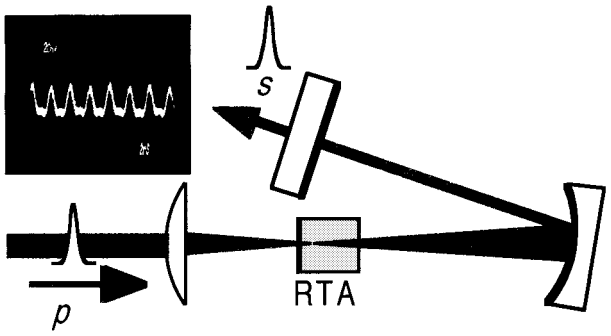

Figure 8. Configuration of the semi-monolithic Ti:sapphire-pumped RTA OPO shown together with the 344 MHz signal pulse sequence recorded by a fast photodiode.

and idler outputs at 344 MHz. A small efficient device of this kind is well suited to pumping by a minilaser-pumped Ti:sapphire system thus providing a compact pump-wavelength-tunable infrared source configuration.

4. Novel characterization techniques for femtosecond pulses

A recent experiment in which the evolution of vibrational wavepackets on an excited state of iodine vapour was studied (Kohler *et al.* 1995), highlighted the importance of determining the frequency chirp of a pulse. Using a negatively chirped pulse, researchers were able to prepare a molecular wavepacket with an internuclear position and momentum of their choice. An oppositely chirped pulse with similar intensity and duration failed to produce a localized wavepacket. Rapid progress in the refinement of advanced femtosecond laser sources together a complementary development of comprehensive pulse characterization methods such as frequency-resolved optical gating (FROG) (Trebino & Kane 1993) have enabled experiments like this to be carried out with quantitative rigour. The FROG technique uses a CCD camera to record a two-dimensional image of the pulse in time and frequency (the FROG trace) which is unique to a particular pulse shape and chirp. A computer algorithm is then used to deconvolve the FROG trace to give the exact intensity envelope and phase of the pulse. A variety of implementations of FROG exist and the experiment referred to above (Kohler *et al.* 1995) used polarization-gated (PG) FROG (Delong *et al.* 1994*a*) which is suitable for low-repetition-rate amplified systems. The emphasis on high pulse-repetition rate systems for time-resolved studies makes it necessary to provide a convenient method of measuring the intensity and phase of a pulse from an oscillator system such as a Ti:sapphire laser or a femtosecond OPO. Second-harmonic generation (SHG) FROG (Delong *et al.* 1994*b*) enables this to be done using a modified autocorrelator. We have developed this technique into a system which permits the real-time monitoring of the FROG trace of a pulse (Reid *et al.* 1997*c*) and we have used it to accurately measure the intensity and phase of a signal pulse from a dispersion-compensated femtosecond OPO based on RTA. A representative FROG trace with the inferred temporal and spectral intensity and phase are included as figure 9. The agreement between the experimentally measured pulse spectrum and that generated by the FROG analysis is excellent and implies that the pulses shown in figure 9 are genuinely representative of those produced by our parametric oscillator.

Simple, convenient and inexpensive methods of pulse characterization are useful when regular monitoring of ultrashort-pulse lasers is required. Second-order auto-

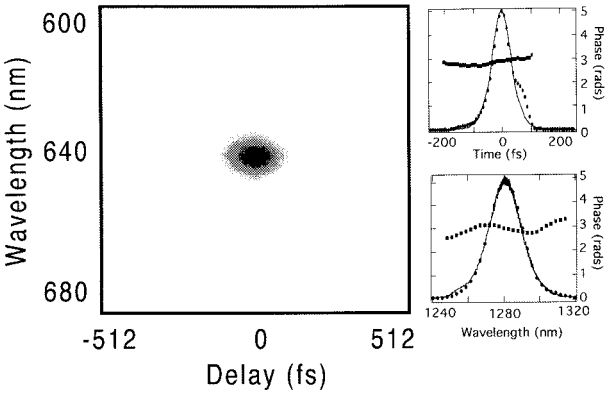

Figure 9. FROG trace (left) and the derived pulse intensity and phase (top, temporal; bottom, spectral). The solid curve superposed on the temporal data is a best-fit $\mathrm{sech}^2(t)$ intensity profile. A pulse spectrum measured independently of the FROG apparatus is superposed on the spectral data to illustrate the excellent agreement between this technique and existing methods of pulse measurement.

correlation involving second-harmonic generation has become the most frequently used technique for measuring the duration and general quality of ultrashort laser pulses and the intensity of the second-harmonic signal is generally detected with a photomultiplier tube. Drawbacks to this implementation of SHG autocorrelation are several and include limitations on the pulse bandwidth imposed by the finite phase-matching bandwidth of the SHG crystal, polarization sensitivity and the need for a high-voltage power supply. In very recent work we have demonstrated that the SHG crystal and photomultiplier tube in an autocorrelator can be replaced without loss of functionality by a light-emitting diode (LED) used as a nonlinear detector. Figure 10 shows the voltage response of an AlGaAs LED to incident picosecond and femtosecond pulses. In each case the response is quadratic and therefore ideally suited for second-order autocorrelation. A fringe-resolved autocorrelation measured using an AlGaAs LED at 1300 nm is shown in figure 11 and the inset shows an intensity autocorrelation measured using the same LED at 800 nm using only 350 μW of average power. The mechanisms and bandwidth of the detection process are discussed briefly elsewhere together with full details of the autocorrelator arrangement (Reid *et al.* 1997*d*). The availability, low cost and convenience of the LED autocorrelator thus makes it attractive to users requiring a simple method for pulse measurement across a range of wavelengths.

5. Summary

The rapid pace of the evolution of femtosecond technology in the 1990s is set to continue into the next century. As pulse durations approach the single optical-cycle limit, new spectroscopic techniqiues will become available which will utilise the wide spectral bandwidth of such pulses to simultaneously excite a large number of molecular and atomic transitions. Single-cycle pulses can be compared to a coherent continuous-wave 'white-light' source suitable for sensitive time-resolved and interferometric spectral measurements. Work in our laboratory aims to demonstrate mid-infrared single-cycle pulses at 3 μm whose bandwidth will exceed 1000 nm and includes a number of important atomic and molecular resonances.

Incorporation of novel nonlinear materials like PPLN into ultrashort-pulse sources

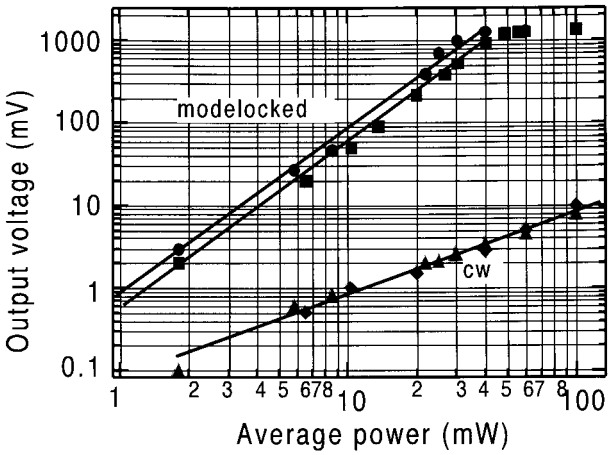

Figure 10. Variation of the output voltage from an AlGaAs LED with average incident power from a Ti:sapphire laser running femtosecond mode-locked (circles), picosecond mode-locked (squares) and continuous wave (diamonds, triangles). The solid lines through the mode-locked data are best fit quadratic profiles (error $< 2\%$) and the line through the cw data is a best-fit linear profile (error $< 5\%$).

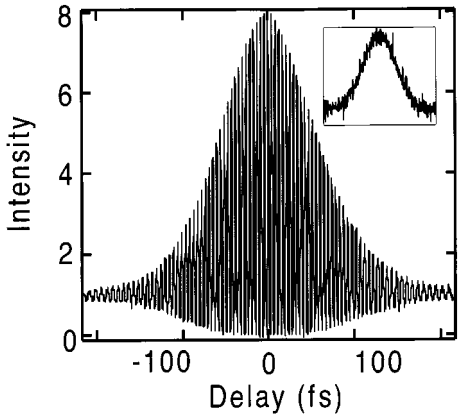

Figure 11. Interferometric autocorrelation recorded at 1300 nm using a Michelson autocorrelator and an AlGaAs LED and (inset) an intensity autocorrelation recorded at 800 nm using the same LED and an incident average power of 350 μW.

promises exciting possibilities because of the potential to use chirped-period poled gratings to engineer exceptional phasematching characteristics such as enhanced conversion bandwidths or intrinsic compensation for intracavity dispersion. Chirped gratings can also be used to simultaneously phasematch two processes which, for example, allows efficient third-harmonic generation in a single crystal and will be important in developing pulse characterization devices suitable for femtosecond oscillators.

Sources for time-resolved studies have matured in recent years to a point where the experiments that can be conceived are no longer 'laser limited'. The wide range of new sources which have evolved combine extensive tunability with efficiency and simplicity not previously available and this development has been matched by new methods which provide complete characterization of pulse intensity and phase. The future promises smaller, more efficient and simpler femtosecond laser sources which

will provide elegant tools for addressing the challenge of investigating the dynamics of chemical and biological systems.

The authors acknowledge the financial assistance of the UK Engineering and Physical Sciences Research Council and British Aerospace Defence PLC and are grateful to Crystal Associates Inc. for the supply of KTA and RTA material and to Dr Dieter Jundt at Crystal Technology Inc. for the supply and fabrication of PPLN. M.E. gratefully acknowledges the support of the Royal Society through a University Research Fellowship.

References

Aoshima, S., Itoh, H. & Tsuchiya, Y. 1997 *Jap. J. Appl. Phys.* **36**, L114.

Baltuska, A., Wei, A., Pshenichnikov, M. S. & Wiersma, D. A. 1997 *Opt. Lett.* **22**, 102.

Bouma, B. E. & Fujimoto, J. G. 1996 *Opt. Lett.* **21**, 134.

Brovelli, L. R., Jung, I. D., Kopf, D., Kamp, M., Moser, M., Kartner, F. X. & Keller, U. 1995 *Electron. Lett.* **31**, 287–289.

Burns, D., Critten, M. P. & Sibbett, W. 1996 *Opt. Lett.* **21**, 477.

Corkum, P. B. 1993 *Phys. Rev. Lett.* **71**, 1994.

Corkum, P. B., Burnett, N. H. & Ivanov, M. Y. 1994 *Opt. Lett.* **19**, 1870.

Critten, M. P., Burns, D. & Sibbett, W. 1996 In *Conf. on Lasers and Electro Optics Europe, Hamburg*, Paper CFF1.

Critten, M. P., Burns, D., Evans, J. M., Lamb, K., Yelland, C. & Sibbett, W. 1996 *J. Mod. Opt.* **43**, 919.

Delong, K. W., Trebino, R. & Kane, D. J. 1994*a* *J. Opt. Soc. Am.* B **11**, 1595.

Delong, K. W., Trebino, R., Hunter, J. & White, W. E. 1994*b* *J. Opt. Soc. Am.* B **11**, 2206.

Dymott, M. J. P. & Ferguson, A. I. 1994 *Opt. Lett.* **19**, 1988.

Dymott, M. J. P. & Ferguson, A. I. 1995 *Opt. Lett.* **20**, 1157.

Ellingson, R. J. & Tang, C. L. 1992 *Opt. Lett.* **17**, 343.

Evans, J. M., Spence, D. E., Sibbett, W., Chai, B. H. T. & Miller, A. 1992 *Opt. Lett.* **17**, 1447–1449.

Falcoz, F., Balembois, F., Georges, P. & Brun, A. 1995 *Opt. Lett.* **20**, 1874.

Fejer, M. M., Magel, G. A., Jundt, D. H. & Byer, R. L. 1992 *IEEE J. Quantum. Electron.* **28**, 2631.

Kafka, J. D., Watts, M. L. & Pieterse, J. W. J. 1992 *IEEE J. Quantum Electron.* **28**, 2151.

Kärtner, F. X., Jung, I. D., Fluck, R., Zhang, G. & Keller, U. 1996 In *Conf. on Lasers and Electro-Optics Europe, Hamburg*, Paper CFF3.

Kim, K. J., Chattopadhyay, S. & Shank, C. V. 1994 *Nucl. Inst. Meth. Phys. Rev.* A **341**, 351.

Kmetec, K. D., Gordon III, C. L., Macklin, J. J., Lemoff, B. E., Brown, G. S. & Harris, S. E. 1992 *Phys. Rev. Lett.* **68**, 1527.

Knox, W. H., Downer, M. C., Fork, R. L. & Shank, C. V. 1984 *Opt. Lett.* **9**, 552.

Kohler, B., Yakovlev, V. V., Che, J., Krause, J. L., Messina, M., Wilson, K., Schwentner, N., Whitnell, R. M. & Yan, Y. 1995 *Phys. Rev. Lett.* **72**, 3360.

Kopf, D., Weingarten, K. J., Brovelli, L. R., Kamp, M. & Keller, U. 1994 *Opt. Lett.* **19**, 2143.

Lamb, K. 1996 Ph.D. thesis, University of St Andrews.

Liu, Y. M., Sun, K. W., Prucnal, P. R. & Lyon, S. A. 1992 *Opt. Lett.* **17**, 1219.

Mellish, R., Barry, N. P., Hyde, S., Jones. R., French, P. M. W., Taylor, J. R., vann der Poel, C. J. & Valster, A. 1995 *Opt. Lett.* **20**, 2312.

Murnane, M. M., Kapteyn, H. C. & Falcone, R. W. 1989 *Phys. Rev. Lett.* **62**, 155.

Myers, L. E., Eckardt, R. C., Fejer, M. M., Byer, R. L., Bosenberg, W. R. & Pierce, J. W. 1995 *J. Opt. Soc. Am.* B **12**, 2102.

Nebel, A. & Beigang, R. 1991 *Opt. Lett.* **16**, 1729.

Pelouch, W. S., Powers, P. E. & Tang, C. L. 1992 *Opt. Lett.* **17**, 1581.

Pshenichnikov, M. S., de Boeij, W. P. & Wiersma, D. A. 1994 *Opt. Lett.* **19**, 572.

Ramaswamy, M., Ulman, M., Paye, J. & Fujimoto, J. G. 1993 *Opt.Lett.* **18**, 1822.

Reid, D. T., McGowan, C., Ebrahimzadeh, M. & Sibbett, W. 1997*a* *IEEE J. Quantum. Electron.* **33**, 1.

Reid, D. T., McGowan, C., Sleat, W. E., Ebrahimzadeh, M. & Sibbett, W. 1997*b* *Opt. Lett.* **22**, 15.

Reid, D. T., McGowan, C., Sleat, W. E. & Sibbett, W. 1997*c* Engineering and laboratory notes. *Optics Photonics News* **8**(5).

Reid, D. T., Padgett, M., McGowan, C., Sleat, W. E. & Sibbett, W. 1997*d* *Opt. Lett.* **22**, 233.

Rizvi, N. H., French, P. M. W. & Taylor, J. R. 1992 *Opt. Lett.* **17**, 279.

Robertson, A., Knappe, R. & Wallenstein, R. 1997 *J. Opt. Soc. Am.* B **14**, 672.

Seas, A., Petricevic, V. & Alfano, R. R. 1992 *Opt. Lett.* **17**, 937–939.

Sennaroglu, A., Pollock, C. R. & Nathel, H. 1994 *Opt. Lett.* **19**, 390–392.

Spence, D. E., Kean, P. N. & Sibbett, W. 1990 *Tech. Dig. CLEO'90 21–25 May 1990, Anaheim CA*, Paper CPDP10.

Spence, D. E., Kean, P. N. & Sibbett, W. 1991*a* *Opt. Lett.* **16**, 42.

Spence, D. E., Evans, J. M., Sleat, W. E. & Sibbett, W. 1991*b* *Opt. Lett.* **16**, 1762.

Stingl, A., Spielmann, C., Krausz, F. & Szipöcs, R. 1994 *Opt. Lett.* **19**, 204.

Strickland, D. & Mourou, G. 1985 *Opt. Commun.* **56**, 219.

Trebino, R. & Kane, D. J. 1993 *J. Opt. Soc. Am.* A **10**, 1101.

Tsuda, S., Knox, W. H. & Cundiff, S. T. 1996 *Appl. Phys. Lett.* **69**, 1538.

Tsuda, S., Knox, W. H., Desouza, E. A., Jan, W. Y. & Cunningham, J. E. 1995 *Opt. Lett.* **20**, 1406–1408.

Valentine, G. J., Kennedy, G. T. & Sibbett, W. 1996 In *Conf. on Lasers and Electro-Optics Europe, Hamburg*, Paper CFF6.

Xu, L., Spielmann, C., Krausz, F. & Szipöcs, R. 1996 *Opt. Lett.* **21**, 1259.

Yanovsky, V. P., Wise, F. W., Cassanho, A. & Jenssen, H. P. 1995 *Opt. Lett.* **20**, 1304–1306.

Zhou, J., Huang, C.-P., Murnane, M. M. & Kapteyn, H. C. 1995 *Opt. Lett.* **20**, 64.

Zhou, J., Taft, G., Huang, C.-P., Murnane, M. M., Kapteyn, H. C. & Christov, I. P. 1994 *Opt. Lett.* **19**, 1149.